Effect of arbuscular mycorrhizal fungi (AMF) and plant growth promoting rhizobacteria (PGPR) on microbial community structure of phenanthrene and pyrene contaminated soils using Illumina HiSeq sequencing

Wen-bin Li[a,§], Wei Li[a,§], Li-jun Xing[a], Shao-xia Guo[a,b,*]

[a]College of Landscape Architecture and Forestry, Qingdao Agricultural University, Qingdao 266109, Shandong. P. R. China.

[b]Institute of Mycorrhizal Biotechnology, Qingdao Agricultural University, Qingdao, 266109, Shandong. P. R. China.

[§]Wen-bin Li and Wei Li contributed equally.

* Corresponding author

phone: +86 0532 86080493 E-mail: gsx2309@126.com

Competing Interests: The authors have declared that no competing interests exist.

Abstract: In order to determine the influence of arbuscular mycorrhizal fungi (AMF, *Glomus versiforme*) and plant growth promoting rhizobacteria (PGPR, *Pseudomonas fluorescens*, PS2-6) on degradation of phenanthrene (PHE) and pyrene (PYR) and the change of microbial community structure in soils planted with tall fescue (*Festuca elata*), four treatments were set up in phenanthrene (PHE) and pyrene (PYR) contamined soil: i.e., tall fescue (CK), AMF + tall fescue (GV), PGPR + tall fescue (PS) and AMF + PGPR + tall fescue (GVPS), PHE and PYR dissipation in the soil and accumulated in the tall fescue were investigated. Our results showed that highest removal percentage of PHE and PYR in contaminated soil as well as biomass of tall fescue were observed in GVPS. PHE and PYR accumulation by tall fescue roots were higher than shoots, the mycorrhizal status was best manifested in the roots of tall fescue inoculated with GVPS, and GVPS significantly increased the number of PGPR colonization in tall fescue rhizosphere soil. And paired-end Illumina HiSeq analysis of 16S rRNA and Internal Transcribed Spacer (ITS) gene amplicons were also employed to study change of bacterial and fungal communities structure in four treatments. GVPS positively affected the speices and abundance of bacteria and fungi in PHE and PYR contaminated soil, an average of 71,144 high quality bacterial 16S rDNA tags and 102,455 ITS tags were obtained in GVPS, and all of them were assigned to 6,327 and 825 operational taxonomic units (OTUs) at a 97% similarity, respectively. Sequence analysis revealed that *Proteobacteria* was the dominant bacterial phylum, Ascomycota was the dominant fungal phylum in all treatments, whereas *Proteobacteria* and *Glomeromycota* were the most prevalent bacterial and fungal phyla in GVPS, respectively. And in the generic level, *Planctomyces* is the richest bacterial genus, and *Meyerozyma* is the richest fungal genus in all treatments, whereas *Sphingomona* was the dominant bacterial genus, while the dominant fungi was *Fusarium* in GVPS. Overall, our findings revealed that application of AMF and PGPR had an effective role in improving the growth characteristics, root colonization of *F. elata* and soil microbial community structure in PHE and PYR contaminated soils, but no obvious in degradation efficiencies of PAHs as compared to the control.

Key words: Arbuscular mycorrhizal fungi (AMF); Plant growth promoting rhizobacteria (PGPR); Synergistic effect; Phenanthrene and pyrene; *Festuca elata.*

1 Introduction

Soil contaminated with polynuclear aromatic hydrocarbons (PAHs) is a major environmental problem worldwide, mainly caused by the incomplete combustion of organic macromolecule substances generally concerning industrial and urban activities (Eremina et al., 2016). PAHs such as phenanthrene (PHE) and pyrene (PYR) have become the most ubiquitous environmental pollutants (Anyanwu et al., 2018). Due to highly mutagenic and carcinogenic properties and are commonly found in soil at high concentrations in many countries, PHE and PYR soil contamination has attracted particular attention (Calonne et al., 2014).

In recent years, new technology employing microorganisms and/or plants to remove PAHs from contaminated soils has been proposed by many researchers (Haritash and Kaushik, 2009; Khan et al., 2013). In situ bioremediation with microorganisms has been recognized as the most cost-effective, reliable, and promising approach for restoration of PHE and PYR contaminated soil (Gao et al., 2011). Among these root associated microorganisms, arbuscular mycorrhizal fungi (AMF) are one of the important rhizosphere microorganisms that participate in beneficial symbiosis with the root system of nearly 80% of terrestrial vascular plants. Besides improving host nutrition AMF are also known to alleviate the plant host from biotic and abiotic stress (Cornejo et al., 2017; Smith and Read, 2010). Recently, AMF have been found to increase soil PAHs dissipation both by promoting the soil microbial population leading to a PAHs biodegradation and via accumulation of PAHs in fungal tissue in roots (Aranda et al., 2013; Cheema et al., 2010; Gao et al., 2011; Wu et al., 2011), and affect the uptake and translocation of PAHs in plants (Wu et al., 2009), indicating the potential of AMF in bioremediation for PAHs contaminated soil. Also, AMF do interact with and modify the microbial communities that the extraradical hyphae encounter in soil, and in this manner they can affect microbial degradation processes indirectly (Joner and Corinne, 2003).

Meanwhile, plant growth promoting rhizobacteria (PGPR), a kind of beneficial bacteria found in the rhizosphere, have also received much interest in the field of phytoremediation, which were utilized to combine plants to remove contaminants from soil (Ahmad et al., 2008; Ma et al., 2015). In recent years, PGPR have been recognized as one of the most effective technologies for decontaminating PAHs-polluted soils (Dong et al., 2014; Yateem and Awatif, 2013). Rao et al. (2015) screened *Bacillus cereus* CPOU13 from soil samples of petroleum contaminated areas can effectively

64 degrade PHE, anthracene and PYR in soil. Inoculation of PAH-degrading bacteria (*Acinetobacter* sp.) resulted in a much
65 higher dissipation (43%–62%) of PYR in the rhizosphere of rice compared with control (6–15%) (Gao et al., 2006).
66 Therefore, AMF, PGPR, and other soil microorganisms that establish mutual symbiosis with the majority of higher
67 plants, can provide positive impacts on plant establishment and survival in contaminated soils. And the activity of
68 rhizosphere microbial community is a major limiting factor in the process of rhizoremediation. However, effects of
69 combined inoculation with AMF and PGPR to mitigate the adverse impacts of PAHs on microbial community and
70 possible bioremediation is limited. By detecting the base sequence of specific genetic substances in soil microbial cells,
71 the complexity and diversity of soil microbial communities can be revealed more comprehensively and accurately, which
72 has been widely used in the study of soil microbial communities (Bokulich and Mills, 2013; Caporaso et al., 2012). And
73 understanding the changes of microbial community structure or enrichment genera related to the biodegradation of PAHs
74 is helpful to deepen the understanding of the theory of rhizoremediation of PAHs-contaminated soils.
75 Traditional molecular fingerprint techniques, such as, denatured gradient gel electrophoresis (DGGE) (Pacwa-
76 Płociniczak et al., 2016), terminal restriction fragment length polymorphism (T-RFLP) (Grant et al., 2010) have great
77 limitations in the analysis of complex microorganisms in PAHs contaminated soil. And high-throughput sequencing has
78 been widely used in rhizosphere microbial diversity research (Sun et al., 2016; Wang et al., 2016). Recent next-generation
79 sequencing (NGS) methods, such as Illumina sequencing techniques, may provide researchers a new way to detect the
80 microbial taxa, especially those with low-abundant species changes (Uroz et al., 2013). However, few studies have
81 attempted to link PAH degradation to the interactive effects of AMF and PGPR on the microbial community composition
82 of soil contaminated with PAHs. Thus the three objectives of this work were: (1) to investigate the effects of dual
83 inoculation AMF and PGPR on microbial community for soils with PHE and PYR pollutants, and (2) the impacts of
84 AMF and PGPR on plant uptake and accumulation of PHE and PYR in soils, and (3) to determine the influence of AMF
85 and PGPR inoculation on the growth of *Festuca* elata in soil contaminated by PHE and PYR were also investigated.
86
87 **2 Materials and Methods**

88 **2.1 Soil**

89 The soil used in this study was collected from natural wasteland harvested from non-farmland (total
90 PAHs<0.2mg • kg^{-1}) in campus of Qingdao Agricultural University, China. The soil has the following basic
91 characteristics: pH(1:2.5 water) 5.62, organic matter 8.6 g • kg^{-1}, total N 0.85 g • kg^{-1}, total P 0.40 g • kg^{-1}, total K 10.7
92 g • kg^{-1}, hydrolyzable N 44mg • kg^{-1}, available P 12.1mg • kg^{-1}, available K 76.3mg • kg^{-1}. 52.1% sand, 27% silt, 20.9%
93 clay and 2.03% soil organic matter. Soil then sieved and mixed with washed sand (1:1). The soil was air-dried and passed
94 through 2mm sieve to remove stones and roots. After being air dried, appropriate concentrations of the mixtures of PHE
95 and PYR (100 mg/kg PHE + 100 mg/kg PYR) were spiked into soil samples to achieve certain PAH concentrations.

96 **2.2 Microbial inocula and host plants**

97 Tall fescue seeds (*Festuca elata* 'Crossfire II') that purchased from Clover Group Co., Ltd., Beijing, China. were
98 surface-disinfected by soaking in 10% (v/v) solution of hydrogen peroxide for 10 min and rinsed with sterile distilled
99 water. Mycorrhizal inoculums of a *Glomus versiforme* strain were the most popular AMF spore in this soil (Li et al.,
100 2013). The AMF inoculums consisted of a mixture of rhizospheric soil from trap cultures (*Trifolium repens*) containing
101 spores, mycelium, sand and root fragments was sieved (<2 mm), that was provided by the Institute of Mycorrhizal
102 Biotechnology of Qingdao Agricultural University. The PGPR bacteria tested were *Pseudomonas fluorescens* Ps2-6,
103 which were cultured in beef extract peptone medium and inorganic salt medium for standby.

104 Surface sterilized seeds were sown in porcelain pots (20 cm in diameter × 25 cm high) containing 3 kg air-dried soil.
105 After germination, the seedlings were thinned to 200 per pot, followed by inoculation with 50 g AMF inoculum and/or
106 10 ml PGPR zymotic fluid (1×10^8 CFU • ml^{-1}). In the non-inoculation treatments, an equivalent amount of radiation-
107 sterilized inoculum was used to provide similar conditions, except for the absence of the instead of the active AMF and/or
108 PGPR inoculation. All the treatments were prepared in decuplicate.

109 All the pots were arranged randomly in a greenhouse, with natural light and day/night temperature of 30/25°C and
110 humidity of 60%±2%. Quarter of the Hoagland solution was supplied regularly and the pots were weighed every week
111 to adjust the water content.

Other samples of roots and shoots were then freeze-dried and ground, in preparation for PAHs analysis. The entire soil in each pot was thoroughly homogenized, ground sufficiently to pass through a 100-mesh sieve, and divided into two sets. One was stored at −20°C for DNA extraction, and the other was stored at 4 °C for PAHs analysis.

2.3 PAH analysis

5 g of freeze-dried soil sample was mixed with 15 ml dichloromethane : acetone (1:1) in a glass centrifuge tube and extracted for 20 min with an Ultrasonic Disrupter, then centrifugation at 3000 rpm for 10 min to precipitate the soil or debris. The supernatant was collected and concentrated into about 2 ml in a rotary evaporator, dissolved in 10 ml n-hexane and loaded on to a column packed with layers of silica gel (200-300 mesh), neutral aluminum oxide (100-200 mesh) and Na_2SO_4 followed by elution with 80 ml hexane and dichloromethane (7:3, v/v) mixture. The filtrate was re-concentrated to 2 ml and further carefully blown dry with nitrogen. The residue was dissolved in 100 μl of n-hexane and filtrated with 0.45 μm-Teflon filter to remove particles prior to analysis. PAHs were analyzed using an Agilent 7890A gas chromatography equipped with a flame ionization detector.

2.4 Mycorrhizal colonization and bacteria number

After a growth period of 60 days, shoots of tall fescue were harvested, and washed with sterile water. Parts of fresh roots were randomly collected from each pot to determine the mycorrhiza infection rate. Mycorrhizal infection rate was calculated with the root segment frequency conventional method of (Biermann and Linderman, 1981), using Eq. (1): $C = Rc/Rt \times 100$, where C (%) is the colonization rate, Rc is the total number of root segments colonized, and Rt is the total number of root segments studies. Relative mycorrhizal dependency was calculated using Eq. (2): $RMD = [(PDWm - PDWn)/ PDWm] \times 100\%$, where RMD is relative mycorrhizal dependency (%), PDWm is mycorrhizal plant dried weight, PDWn is non-inoculated plant dried weight.

The aerobic PAH-degrading bacteria in soil are enumerated over basal mineral medium agar plates (g • L^{-1}: NH_4Cl 1.0, K_2HPO_4 0.3, KH_2PO_4 0.2, $MgSO_4$ 0.5, pH 7.2) containing 100mg • L^{-1} Phe, and 50 mg • L^{-1} of cycloheximide for suppression of fungal growth. There are three replicates for each dilution, and all plates were incubated at 28 °C. The colonies formed were counted after 2 weeks of incubation, and the number is expressed as CFU • g^{-1} dry soil.

136 **2.5 Soil DNA extraction**

137 Before DNA extraction, the sample was mixed thoroughly. Then the samples were ground with liquid nitrogen to
138 avoid inhomogeneity. The total genomic DNA of the samples was extracted from 10 g of soil using the E.Z.N.A. stool
139 DNA Kit (Omega Bio-tek, Norcross, GA, U.S.), according to the manufacturer's protocols. The DNA quality was assayed
140 using a NanoDrop spectrophotometer (Thermo Fisher Scientific, USA) and by agarose gel electrophoresis. The
141 absorption ratio at 260/280 nm was required to be within the range of 1.8~2.0. Extracted DNA was diluted to 1 ng • μl^{-1}
142 and stored at -20 °C until further processing.

143 **2.6 PCR amplification and sequencing**

144 Diluted DNA from each sample was used as a template for PCR amplification of bacterial 16S and fungal ITS rRNA
145 gene sequences with barcoded primers and HiFi Hot Start Ready Mix (KAPA). To determine the diversity and structure
146 of the bacterial communities in different samples, the universal primer set 341F (5'-CCTACGGGNGGCWGCAG-3')
147 and 806R (5'-GGACTACHVGGGTATCTAAT-3') was used to amplify the V3-V4 regions of the 16S rRNA genes, with
148 a 8 bp barcode on the reverse primer. And the universal primer set KYO2F (5'-GATGAAGAACGYAGYRAA-3') and
149 ITS4R (5'-TCCTCCGCTTATTGATATGC-3') was used to amplify the ITS2 variable regions for fungal-diversity
150 analysis. PCR reactions were performed in triplicate 50 μL mixture containing 5 μL of 10 × KOD Buffer, 5 μL of 2.5
151 mM dNTPs, 1.5 μL of each primer (5 μM), 1 μL of KOD Polymerase, and 100 ng of template DNA. Cycling conditions
152 involved an initial 2 min denaturing step at 95 °C, followed by 27 cycles of 10 s at 98 °C, 30 s at 62 °C and 30 s at 68 °C,
153 and a final extension phase of 10 min at 68 °C.

154 Amplicons were extracted from 2% agarose gels and purified using the AxyPrep DNA Gel Extraction Kit (Axygen
155 Biosciences, Union City, CA, U.S.) according to the instructions and quantified using QuantiFluorTM (Promega, U.S.).
156 Purified amplicons were pooled in equimolar and paired-end sequenced (2×250bp) on an Illumina Hiseq2500 platform
157 according to the standard protocols.

158 **2.7 Processing and analyzing of sequencing data**

159 Raw Illumina fastq files were de-multiplexed, quality filtered, and analysed using QIIME (version 1.17) (Caporaso

et al., 2010) with the following criteria: 1) Removing reads containing more than 10% of unknown nucleotides (N); 2) Removing reads containing less than 80% of bases with quality (Q-value)＞20; 3) Paired end clean reads were merged as raw tags using FLSAH (v 1.2.11) (Magoc, 2011) with a minimum overlap of 10bp and mismatch error rates of 2%; 4) Noisy sequences of raw tags were filtered by QIIME (V1.9.1) (Caporaso et al., 2010). Reads that could not be assembled were discarded. Operational taxonomic units (OTUs) with ≥ 97 % similarity using UPARSE (version 7.1), and chimeric sequences were identified and removed using UCHIME algorithm (http://www.drive5.com/usearch/manual/uchime_algo.html). Chao1, Simpson and Shannon diversity indices were calculation in QIIME. OTU rarefaction curve and Rank abundance curves was plotted in QIIME. Statistics of between group Alpha index comparison was calculated by a Welch's t-test and a Wilcoxon rank test in R. Alpha index comparing among groups was computed by a Tukey's HSD test and a Kruskal-Wallis H test in R. The beta diversity analysis was performed using UniFrac (Lozupone et al., 2011). The principal component analysis (PCA), Venn diagrams and Heatmap figures were calculated and plotted in R.

2.8 Statistical analysis

All data were analyzed with Excel 2010 and SPSS11.5. All data were first analyzed by analysis of variance (ANOVA) to determine significant differences for the treatment effects ($P = 0.05$). Significant differences between individual means were determined using Duncan's Multiple Range Test ($P = 0.05$). Data points in Fig. 1 represent the means ± SE of three independent experiments with at least three replications per treatment.

3 Results

3.1 Promotion of AMF and PGR on the growth of *F. elata* and removal of PHE and PYR in soil

The effect of the inoculation of PGPR and/or AMF on the growth of in different treatment soils was investigated after 60 days experiment in greenhouse condition. Compared with the CK, *F. elata* inoculated with GV, PS, and GVPS produced larger fresh weight, dry weight and higher plant height under PHE and PYR stress conditions, however, the GV and PS did not have an effect on tiller number of *F. elata*. Moreover, the GVPS treatment produced the highest fresh weight (0.56 ± 0.03) g, dry weight (0.1177 ± 0.003) g and plant height (36.7 ± 0.8) g ($p<0.05$) in the concentration of

184 PHE and PYR at 100 mg • kg^{-1}, and the fresh weight, dry weight and height of plant increased by 1.43-fold, 93.90% and
185 51.03% compared with that of CK, respectively (Table 1).

186 The mycorrhizal status was best manifested in the roots of plants inoculated with GVPS, the percentage of root
187 mycorrhizal colonization of GVPS treatment was 69% (Fig. 1). GVPS treatment significantly increased the number of
188 PGPR colonization in tall fescue rhizosphere soil. the number of PGPR reached a maximum of 9.5×10^7 CFU • g^{-1} at 100
189 mg • kg^{-1} of PHE and PYR. Meanwhile, the GVPS treatment significantly enhanced hyphal density, entry point number,
190 and mycorrhizal relative dependence ($p < 0.05$, Fig. 1), the hyphal density, entry point number, and mycorrhizal relative
191 dependence of GVPS increased by 75%, 73% and 383%, respectively, however, did not significantly ($p < 0.05$) increased
192 the colonization, spore density, vesicle number, and arbuscule colonization of tall fescue (Fig. 1). By the end of the
193 experiment, the PHE concentrations decreased from the initial value of 100 mg • kg^{-1} to 2.85, 2.85, 2.84, and 2.46
194 mg • kg^{-1} dry soil in CK, GV, PS and GVPS, respectively, corresponding to degradation efficiencies of 97.10%, 97.10%,
195 97.10%, and 97.50%, respectively. The PYR concentrations decreased from the initial value of 100mg • kg^{-1} to 10.12,
196 8.72, 8.92 and 5.11 mg • kg^{-1} dry soil in treatments CK, GV, PS and GVPS, respectively, corresponding to removal
197 efficiencies of 89.67%, 91.10%, 90.90% and 94.80%, respectively. Residual concentrations of PHE and PYR in tall
198 fescue shoots and roots are also shown in Table 2. High concentrations of PHE and PYR were detected in tall fescue
199 roots (but not in shoots), root concentrations of PHE in tall fescue grown for 60 days in soils with GV, PS, and GVPS
200 inoculation were 22.62%, 31.13%, 53.63% higher than those of CK, and root concentrations of PYR in tall fescue grown
201 for 60 days in soils with GV, PS, and GVPS inoculation were 56.95%, 30.21%, 67.11% higher than those of CK.
202 Concurrently, PHE and PYR concentrations of shoots in contaminated soil vaccinated with GV, PS and GVPS were
203 significantly ($p < 0.05$) higher than those of CK (Table 2).

204 **3.2 Evaluation of sequencing results of soil microbial library**

205 After sequencing the original data, the low-quality data or non-biologically meaningful data (such as chimeras) are
206 removed to ensure the statistical reliability and biological validity of subsequent analysis. The sequencing run of 16S
207 rRNA amplicons yielded an average of 68,534.67 ± 10,870.14, 69,611 ± 7,337.083, 72,296.333 ± 9,922.511, and 71,144

± 1,136.746 clean tags (per sample), with 4,916, 5,164, 5,570 and 6,327 total OTUs from the CK, GV, PS and GVPS samples, respectively (Table 3). The sequencing run of ITS amplicons yielded 96023 ± 2098.435, 92420.67 ± 8008.382, 100643.3 ± 2112.008, and 102455 ± 6585.639 clean tags, with 595, 649, 783, and 825 total OTUs from the CK, GV, PS and GVPS samples, respectively (Table 3).

The total number of OTUs detected at 97% shared sequence similarity was very high in PHE and PYR contaminated soil, both in terms of bacteria and fungi, and the estimated α-diversities indicated abundant microbial diversity was present in all samples. For bacteria, the number of different phylogenetic OTUs ranged from 1,639 to 2,109, with dual inoculation (GVPS) showing higher 16S rRNA gene diversity than single inoculation (GV, PS) and control group (CK). GVPS presented the highest number of OTUs and bacterial diversity, whereas CK samples had the lowest. For fungi, the number of different phylogenetic OTUs in all samples ranged from 198 to 275 with GVPS exhibiting higher diversity than CK, GV and PS. The GVPS displayed the highest Shannon index and number of OTUs, whereas CK samples had the lowest (Table 3).

Venn diagrams were performed in R, based on the shared OTU tables from 4 different soil groups (Fig. 2A). The total number of unique bacterial OTUs was 3,415, of which 119 OTUs were shared between PS and GVPS treatments, 187 were associated only with treatment of GV (GV, GVPS), and 1035 were shared by all samples (Fig. 2A). Furthermore, in terms of fungi, 504 different OTUs were identified, both PS vs GVPS and GV vs GVPS groups, shared only 46 and 21 OTUs, respectively, and 92 were shared by all samples (Fig. 2B).

3.3 Analysis of microbial community structure

All valid reads were classified from the phylum to the genus level using the default settings in QIIME. The bacterial and fungal communities from the 12 samples were analyzed at phylum, family and genus levels. In total, all the bacteria and fungal identified were classified into 28 and 6 phyla, respectively. *Proteobacteria*, *Saccharibacteria* and *Parcubacteria* were the dominant bacterial phyla, while *Ascomycota*, *Chytridiomycota* and *Basidiomycota* were the dominant fungal phyla. And all the treatments shared similar bacterial and fungal communities, Most samples from the same group shared high similar bacterial communities at all classification levels.

232 At phylum level, the CK, GV, PS and GVPS samples shared common phyla, *Proteobacteria* was the most prevalent
233 bacteria phylum, while different proportions of valid reads from 33.80% to 41.73% were observed for all treatments.
234 More *Proteobacteria* taxa (41.73%) were detected in GVPS than in GV, PS and CK (Fig. 3A). Fungal classification
235 results showed that the dominant phylum was *Ascomycota*, accounting for 33.13–52.04% of all valid reads, with an
236 average relative abundance of 43.56%. The next most dominant fungal phyla were *Chytridiomycota* (average abundance
237 12.13%) and *Basidiomycota* (average abundance 6.60%), and the abundance of *Glomeromycota* (0.27%) in GVPS was
238 significantly higher than that in GV, PS and CK treatment (Fig. 3B).

239 The most prevalent bacterial families detected in all 12 groups included *Xanthomonadaceae* (7.40%-12.58%),
240 *Planctomycetaceae* (average abundance 6.25%), and *Sphingomonadaceae* (average abundance 3.59%). The abundance
241 of *Xanthomonadaceae* (12.58%), *Phytophthoraceae*(6.76%) and *Sphingomycidae*(4.43%) in GVPS was significantly
242 higher than others (Fig. 3C). At the family level, according to the classification of fungi, *Debaryomycetaceae* (average
243 abundance 17.46%) is the richest fungus family in all samples, accounting for 9.94% - 27.67% of the total.
244 *Spizellomycetaceae* is the second most abundant fungal family with an average abundance of 12.12%. The proportion of
245 *Nectriaceae* (11.76%), *Pseudoglobulaceae* (4.44%) and *Cladosporidae* (1.08%) were significantly higher in GVPS
246 samples compared to other samples (Fig. 3D).

247 At the generic level, according to the results of bacterial taxonomy, *Planctomyces* is the richest genus in all samples,
248 accounting for 3.0% - 3.39% of the total. *Sphingomonas* is the second most abundant bacteria genus with an average
249 abundance of 2.36%. The other major bacterial genera were *Mycobacterium* (average abundance 2.31%), *Arenimonas*
250 (average abundance 1.92%), *Pseudomonas* (average abundance 1.75%), and *Pirellula* (average abundance 1.53%). The
251 abundance of *Sphingomonas* (3.17%), *Pseudomonas* (2.05%) and *Piriformis* (1.79%) in GVPS was significantly higher
252 than that in other treatments (Fig. 3E). At the generic level, according to the classification of fungi, *Meyerozyma* is the
253 richest fungi genus in all samples, accounting for 9.94% - 27.67% of the total. *Spizellomyces* is the second most abundant
254 fungi genus with an average abundance of 12.12%. The other dominant fungal genera were *Gibberella* (average
255 abundance 4.14%), *Fusarium* (average abundance 3.93%), *Serendipita* (average abundance 3.17%), *Alternaria* (average

256 abundance 2.93%), *Aspergillus* (average abundance 2.09%) and *Chalastospora* (average abundance 0.88%). The
257 abundance of *Fusarium* (8.65%), *Alternaria* (4.09%) and *Cladosporium* (1.07%) in GVPS treatment was significantly
258 higher than other treatments (Fig. 3F). Heatmap clustering analysis results revealed that *Planctomyces*, *Mycobacterium*
259 bacterial genera had high abundances in the CK, GV, and PS, but the *Sphingomonas*, *Planctomyces*, and *Arenimonas*
260 genera had a relatively high abundance in the GVPS (Fig. 4A). For fungi, heatmap clustering analysis showed that
261 *Meyerozyma* and *Spizellomyces* fungus genera had relatively high abundances among all the treatments, while Fusarium
262 had a high abundances in GVPS (Fig. 4B). These finding were consistent with previous results (Fig. 3).

263 **3.4 Effects of AMF and PGPR on soil microbial community richness and diversity in the root zone of *F. elata***

264 The rarefaction curve can evaluate whether the sequencing quantity is sufficient to cover all groups and indirectly
265 reflect the species richness in the treatmens. Rarefaction curves of four treatments (CK, PS, GV, GVPS) for bacteria and
266 fungi are shown in Fig. A.1. None of the rarefaction cure is not parallel with the x-axis, the rarefaction curves of bacteria
267 and fungi calculated at 97% levels showed that the order of OTUs numbers from high to low among samples both were
268 GVPS > PS > GV > CK. And the OTU densities of GVPS was higher than the other three treatments (Fig. A.1). The
269 bacteria and fungi richness based on rarefaction curves were strongly supported by statistical diversity estimates, based
270 on the abundance results of OTUs, the Alpha diversity of each sample was calculated by QIIME software, including
271 Chao 1 value, ACE value, Shannon index and Simpson index (Table 3). The results showed that the values of Chao 1
272 and ACE of GVPS treatment were higher, which indicated that the richness of microbial community under GVPS
273 treatment was higher. And the Simpson diversity index of the four treatments had little difference, indicating that the
274 uniformity of the four treatments and the dominant OTU of the community were similar, while GVPS treatment had the
275 same dominant OTU. Shannon diversity index was higher in GVPS treatment, which indicated that the microbial
276 community in GVPS treatment was richer and contained more rare OTUs (Table 3). Based on the relative abundance of
277 the genera from Fig. 5, the genera with an average abundance of >1 % in at least one group were defined as dominant.

278 To further compare the microbiota among different samples, principal component analysis (PCA) was used to
279 identify the community structure differences under different treatments (Fig. 5). The data are presented as a 2-dimensional

plot to better illustrate the relationship among treatments. At OTU level, PCA demonstrated that four treatments of 12 soil samples were clustered. In bacteria, Except for CK-1 and GV-3, microorganism communities in most treatments gathered together, PCA demonstrated that different soil samples from groups CK and PS gathered together than others. In addition, the GV samples had a relatively higher PC1 value, followed by PS and GVPS treatment, whereas the CK samples had a higher PC2 value at OTU level (Fig. 5A). In fungi, the GVPS groups had a relatively higher PC1 value, followed by PS and CK, while the samples from GV were closer than the other groups. Meanwhile, No significant gathering were observed among four groups (Fig. 5B).

UPGMA clustering obtained a phylogenetic tree by using unweighted group averaging method (Fig. A.2.). Result indicates that same type of samples showed high similarity of bacterial communities (Fig. A.2-A), while similarity of fungal communities from the same treatment is relatively weaker (Fig. A.2-B).

Discussion

Microorganisms such as fungi and bacteria are widely distributed in urban soil, the symbiosis between them provides an ecological basis for screening and establishing bioremediation technology based on the interaction between specific fungi and bacteria (Boer et al., 2010; Pennisi, 2004).Greenhouse experiment was conducted to evaluate the potential effectiveness of a tall fescue, AMF (*Glomus versiforme*, Gv), and PGPR (*Pseudomonas fluorescens*, PS 2-6) symbiosis for remediation of PHE and PYR polluted soil. Tall fescue has been commonly selected to phytoremediation of contaminated soils for its rapid growth characters, vigorous root system, contaminant-tolerant and the demonstrated fast removal of PAHs from polluted soil. For all this, phytoremediation alone may not be a viable technology for many PAHs (Chaudhry et al., 2005), and their synergistic effect between plants and rhizosphere microorganisms to dissipate PAHs, is considered as a promising, cost-effective, and eco-friendly technique to clean up polluted soils (Shahsavari et al., 2015). Previous studies have shown that AMF establish a mutualistic symbiotic relationship with the roots of most plant species. While receiving photosynthates from the plants, AMF promote plant growth and create a very highly surface area that helps to improve the mineral nutrition of the plant and also play a central role in the natural attenuation of toxicity in their hosts (Eke et al., 2016; Lehmann et al., 2014). Meanwhile, PGPR have also been used as inocula to further increase plant

304 growth, and reduce environmental stress (Khan et al., 2013). In this study, GV and PS had a beneficial impact on each
305 other in the plant-AMF-PGPR triple symbiosis. Firstly, inoculation of soil with GV, PS, or GVPS significantly increased
306 fresh, dry weight and height of tall fescue in PHE and PYR polluted soil, and a analogous pattern was reported in previous
307 research (Dong et al., 2014), which showed higher fresh and dry weight of *Avena sativa* inoculated with *Serratia*
308 *marcescens* BC-3 alone or mixed with *Rhizophagus intraradices* than those of the control in petroleum hydrocarbon
309 polluted soil. And two wheat cultivars inoculated with the *Rhizophagus irregularis* and the *Pseudomonas putida* KT2440,
310 dramatically enhance plant growth, and root shoot ratio (Pérezdeluque et al., 2017). It seems that PS acted as helper
311 bacteria in this study, which significantly elevated the plant biomass. However, dual inoculation with PGPR and AMF
312 did not always act as plant growth promoters, a previous founding showed that dual inoculation with *R. irregularis* and
313 Trichoderma viride resulted in plant growth suppression compared to single inoculation with *R. irregularis* (Herrera-
314 Jiménez et al., 2018), therefore, we speculate that the positive effect of AMF+ PGPR depending on the bacterial and
315 fungal type and plant species.

316 Our results also indicated that GV, PS and GVPS significantly removed PHE and PYR in soil and enhanced PHE
317 and PYR accumulation in plants. The highest dissipation rates (PHE: >97%; PYR: 89.67%–94.8%) were detected in
318 treatments of GVPS, and the shoots and roots of tall fescue can absorb 2-6% of PHE and PYR in soil. And plant roots
319 interact closely with soil microorganisms, the positive rhizosphere effect of tall fescue on PHE and PYR removal is
320 primarily due to the enhancement in the microbial activity and the dynamics of bacterial communities. Some researchers
321 considered that higher removal efficiencies of PAHs are often observed in plant rhizospheres than in the non-rhizosphere
322 or unplanted soils (Kawasaki et al., 2016; Kong et al., 2018). Our result showed that inoculation with GV, PS or GVPS
323 can enhance the removal ability of PHE and PYR in soils. A large number of pot and field experiments have reported
324 success in total petroleum hydrocarbon utilizing PGPR inocula and plants (Agarry et al., 2013; Liu et al., 2013). The
325 degradation rate of total petroleum hydrocarbons with PGPR *Serratia marcescens* BC-3 and AMF *Glomus intraradices*
326 co-inoculation treatment was up to 72.24 % (Dong et al., 2014). And the triple symbiosis among rhizobia, AMF and
327 *Sesbania cannabina* help to enhanced PAHs degradation via stimulating both microbial development and soil enzyme

328 activity (Ren et al., 2017). However, we did not notice significantly raised PHE and PYR dissipation in soil planted with
329 tall fescue inoculated by GV, PS, or GVPS as the dissipation rate had already reached 90% in CK, we speculate that the
330 dissipation of PHE and PYR in CK is closely related to the activity of indigenous microbial population. Nevertheless, we
331 still believe significant interactions among tall fescue, GV and PS in promoting PHE and PYR dissipation, since
332 inoculation can altered the structure, density and activity of soil microbial communities (Corgié et al., 2006). In addition.
333 *P. fluorescens* could enhance the *G. versiforme* mycorrhizal relative dependence in the presence of PHE and PYR, and
334 the percentage of root colonization in GVPS was significantly higher than that of GV. Previous studies have shown that
335 the presence of rhizobacterial inoculation might have assisted in the germination of a large number of spores thus leading
336 to a higher AMF infection percentage. Some endophytic species of PGPR were known to excrete cellulase and pectinase
337 (Kovtunovych et al., 1999; Verma et al., 2001) and these enzymatic activities would no doubt aid in mycorrhizal infection.
338 In the meantime, inoculation of *G. versiforme* significantly increased the number of *P. fluorescens* in contaminated
339 soil.

340 At last, high throughput sequencing analyses showed that different inoculation treatments significantly affected the
341 microbial community structure in tall fescue rhizosphere soil polluted by PHE and PYR. The microbial community
342 diversity of PHE and PYR contaminated soil under GVPS treatment was higher than that of GV or PS. The results
343 revealed that the relative abundances of bacterial and fungal phyla (Fig. 3A, B). For bacteria, we observed that
344 *Proteobacteria* (41.73%) were the most abundant bacterial phyla in GVPS (Fig. 3A). *Proteobacteria* have been
345 previously proved to be the most influential on the biodegradation of petroleum contaminated soil (Shahi et al., 2016),
346 previous findings are in line with *Proteobacteria* having a fast-growth phenotype among rhizosphere bacteria and being
347 capable of utilizing a broad range of root-derived carbon substrates (Gomes et al., 2001; Sharma et al., 2005). And in the
348 genus level, *Planctomyces*, *Sphingomonas* and *Mycobacterium* were identified as the main genus in all samples, whereas
349 *Sphingomonas* (3.17%), *Pseudomonas* (2.05%) and *Piriformis* (1.79%) were more frequent in GVPS treatment (Fig. 3E,
350 F). Many previous findings have demonstrated *Sphingomonas* and *Pseudomonas* that plays important roles in the health
351 of plants and enhancing the biodegradation of PAHs (Bacosa and Inoue, 2015; Hayward et al., 2010), and the bacterial

352 community dynamics of the soils indicate that the *Sphingomonas* may play a key role in the early degradation of PAHs
353 (Bacosa and Inoue, 2015; Sara et al., 2014; Singleton et al., 2011). *Pseudomonas* species have also been described as
354 ubiquitous rhizobacteria and have a strong ability to degrade HMW-PAHs in soil. Pseudomonas (Bands 1, 6 and 7) are
355 able to use HMW-PAHs as sources of carbon and energy (Folwell et al., 2016), our results indicating that the increase in
356 *Sphingomonas* and *Pseudomonas* may cause soil stronger endurance. Among microorganisms, some fungi
357 *Glomeromycota* have been found to play important roles in rhizoremediation of PHE and PYR contaminated soil.Some
358 members of *Glomeromycota* have been considered generally as obligate symbiotic fungi, and the *Glomeromycota* phyla
359 can respond rapidly to rhizodeposits (Hannula et al., 2012; Philippe et al., 2007). Previous data showed that members of
360 the *Glomeromycota* phylum depend on carbon and energy derived from plant synthesis to survive, and shares a symbiotic
361 relationship with the roots of plants (Hannula et al., 2012; Lu et al., 2004). Among the fungi identified in our samples,
362 the abundance of *Glomeromycota* was more abundant in GVPS treatment, thus, we speculate that the *Glomeromycota*
363 phylum may also affect symbiosis and interactions between ramie roots and soil microbes, considering that it was highly
364 enriched in the tall fescue rhizosphere. For fungus in the genus level, the abundance of *Fusarium* (8.65%) in GVPS
365 treatment was significantly higher than other treatments (Fig. 3F), and the ability of *Fusarium* spp. to degrade some
366 recalcitrant substances has also been reported, *Fusarium* sp. produced the most significant effect on degradation of HMW-
367 PAHs, giving an overall removal rate of over 30% for 5- and 6-ring PAHs (Potin et al., 2004), and combination of
368 *Fusarium* sp. ZH-H2 and bromegrass offers a suitable alternative for phytoremediation of aged PAH-contaminated soil
369 in coal mining areas (Shi et al., 2017). Accordingly, we believe that the relatively high abundance of *Proteobacteria* and
370 *Fusarium* may function in dissipation of PHE and PYR, thereby, and some species of *Proteobacteria* and *Fusarium* may
371 serve as beneficial microorganisms in the rhizosphere of tall fescue for promoting plant growth. Interestingly, we
372 analyzed the diversity of tall fescue rhizospheric soil according to richness (Chao 1 and ACE) and diversity (Shannon
373 and Simpson) indices, which showed marked changes between GV, PS, GVPS and CK treatment, diversity indices
374 indicated that the diversity of fungal and bacterial community in GVPS were significantly higher than GV, PS and CK
375 in soils, and the result of PCA revealed that fungal community changes in the contaminated-soils are more complex than

bacteria community changes in soil (Fig. 2 and Table 1). Alternatively, the presence of plant promoted the dissipation of PAHs and changed the diversity of active bacterial communities in soil (Guo et al., 2017). However, plants are only the secondary factors affecting microorganism diversity in contaminated soil (Yergeau et al., 2014). And AMF inoculation significantly influenced the development of fungal and bacterial rhizosphere community diversity (Solísdomínguez et al., 2011). Some previous studies deem that the shifts in bacterial community diversity may be due to the different growth responses of soil bacteria to PAHs, and also depends on soil types and plant species (Bacosa and Inoue, 2015; Kawasaki et al., 2016). Furthermore, The soil microbial community diversity is related to the removal of PAHs from contaminated environments (Sawulski et al., 2014), in our study, the removal rates of PHY and PYR were the highest under GVPS treatment, which was consistent with previous reports. In addition, the presence of some specific compounds also contribute to the soil microorganisms diversity. Glomalin is secreted protein by AMF hyphae can stabilizes soil aggregates and increases the hydrophobicity of soil particles, what is important for the fate of PAHs in soil (Augé, 2004; Rillig and Steinberg, 2002). Glomalin may also exceed soil microbial biomass and abundance of microorganisms (Rillig et al., 2001). Thus, we speculated that changes in the bacterial diversity were related to the inoculation of microorganisms or combination effect of plant and microorganisms. In summary, to better understand such interaction and impact of GV and PS on soil microbes, more samples should be taken gradually to provide systematic and detail results on microbial communities.

Conclusion

In conclusion, a detailed picture of bacterial and fungal community variations in PHE and PYR polluted soils under four treatments (CK, GV, PS and GVPS) were analyzed based on the high throughput Illumina sequencing method. The results reflected the significant contribution of GVPS in increasing the speices and abundance of bacteria, whereas no significant differences were observed for fungi in PHE and PYR contaminated soil, meanwhile, the highest dissipation rates of PHE and PYR as well as biomass of tall fescue in GVPS were observed. And tall fescue associated with GVPS significantly ($p < 0.05$) enhanced dissipation of PHE and PYR from soil, PHE and PYR accumulation by tall fescue roots were higher than shoots. Sequence analysis revealed that *Proteobacteria* and *Glomeromycota* were the most prevalent

400 bacterial and fungal phyla in GVPS, respectively. And in the generic level, *Sphingomona* was the dominant bacterial
401 genus, while the dominant fungi was *Fusarium* in GVPS. GVPS had an effective role in improving the growth
402 characteristics, root colonization of *F. elata* and soil microbial community structure in PHE and PYR contaminated soils,
403 but no obvious degradation efficiencies of PHE and PYR as compared to the control.
404

405 **Author contributions**

406 GSX conceived and designed the experiments. LWB, LW and XLJ performed the experiments and analyzed the data. LW

407 wrote the paper.

408

409 **Reference**

410 Agarry, S. E., et al., 2013. Kinetic modelling and half-life study on bioremediation of soil co-contaminated with lubricating
411 motor oil and lead using different bioremediation strategies. Journal of Soil Contamination. 22**,** 800-816.
412 Ahmad, F., et al., 2008. Screening of free-living rhizospheric bacteria for their multiple plant growth promoting activities.
413 Microbiological Research. 163**,** 173-181.
414 Anyanwu, I. N., et al., 2018. Impact of nitrogen-polycyclic aromatic hydrocarbons on phenanthrene and benzo[a]pyrene
415 mineralisation in soil. Ecotoxicology & Environmental Safety. 147**,** 594-601.
416 Aranda, E., et al., 2013. Role of arbuscular mycorrhizal fungus *Rhizophagus custos* in the dissipation of PAHs under root-organ
417 culture conditions. Environmental Pollution. 181**,** 182-189.
418 Augé, R. M., 2004. Arbuscular mycorrhizae and soil/plant water relations. Canadian Journal of Soil Science. 84**,** 373-381.
419 Bacosa, H. P., Inoue, C., 2015. Polycyclic aromatic hydrocarbons (PAHs) biodegradation potential and diversity of microbial
420 consortia enriched from tsunami sediments in Miyagi, Japan. Journal of Hazardous Materials. 283**,** 689-697.
421 Biermann, B., Linderman, R. G., 1981. Quantifying vesicular-arbuscular mycorrhizae: a proposed method towards
422 standardization. New Phytologist. 87**,** 63-67.
423 Boer, W. D., et al., 2010. Living in a fungal world: impact of fungi on soil bacterial niche development. Fems Microbiology
424 Reviews. 29**,** 795-811.
425 Bokulich, N. A., Mills, D. A., 2013. Improved selection of internal transcribed spacer-specific primers enables quantitative,
426 ultra-high-throughput profiling of fungal communities. Appl Environ Microbiol. 79**,** 2519-2526.
427 Calonne, M., et al., 2014. Polyaromatic hydrocarbons impair phosphorus transport by the arbuscular mycorrhizal fungus
428 Rhizophagus irregularis. Chemosphere. 104**,** 97-104.
429 Caporaso, J. G., et al., 2010. QIIME allows analysis of high-throughput community sequencing data. Nature Methods. 7**,** 335-
430 336.
431 Caporaso, J. G., et al., 2012. Ultra-high-throughput microbial community analysis on the Illumina HiSeq and MiSeq platforms.
432 The ISME journal. 6**,** 1621.
433 Chaudhry, Q., et al., 2005. Utilising the synergy between plants and rhizosphere microorganisms to enhance breakdown of
434 organic pollutants in the environment (15 pp). Environmental Science & Pollution Research. 12**,** 34-48.
435 Cheema, S. A., et al., 2010. Degradation of phenanthrene and pyrene in spiked soils by single and combined plants cultivation.
436 Journal of Hazardous Materials. 177**,** 384-389.
437 Corgié, S. C., et al., 2006. Biodegradation of phenanthrene, spatial distribution of bacterial populations and dioxygenase
438 expression in the mycorrhizosphere of *Lolium perenne* inoculated with *Glomus mosseae*. Mycorrhiza. 16**,** 207-212.
439 Cornejo, P., et al., 2017. Contribution of inoculation with arbuscular mycorrhizal fungi to the bioremediation of a copper
440 contaminated soil using *Oenothera picensis*. Journal of soil science and plant nutrition. 17**,** 14-21.
441 Dong, R., et al., 2014. Effect of PGPR *Serratia marcescens* BC-3 and AMF *Glomus intraradices* on phytoremediation of
442 petroleum contaminated soil. Ecotoxicology. 23**,** 674.
443 Eke, P., et al., 2016. Mycorrhiza consortia suppress the fusarium root rot (*Fusarium solani* f. sp. Phaseoli) in common bean (
444 *Phaseolus vulgaris* L.). Biological Control. 103**,** 240-250.
445 Eremina, N., et al., 2016. Distribution of polychlorinated biphenyls, phthalic acid esters, polycyclic aromatic hydrocarbons and
446 organochlorine substances in the Moscow River, Russia. Environmental Pollution. 210**,** 409-418.
447 Folwell, B. D., et al., 2016. Characterisation of biofilm and planktonic bacterial and fungal communities transforming high
448 molecular weight polycyclic aromatic hydrocarbons. Applied & Environmental Microbiology. 82**,** AEM.03713-15.
449 Gao, Y., et al., 2011. Arbuscular mycorrhizal phytoremediation of soils contaminated with phenanthrene and pyrene. Journal of
450 Hazardous Materials. 185**,** 703-709.
451 Gao, Y., et al., 2006. Interactions of rice (*Oryza sativa* L.) and PAH-degrading bacteria (*Acinetobacter* sp.) on enhanced

452 dissipation of spiked phenanthrene and pyrene in waterlogged soil. Science of the Total Environment. 372**,** 1-11.
453 Gomes, N. C. M., et al., 2001. Bacterial diversity of the rhizosphere of maize (*Zea mays*) grown in tropical soil studied by
454 temperature gradient gel electrophoresis. Plant & Soil. 232**,** 167-180.
455 Grant, R., et al., 2010. Microbial community changes during the bioremediation of creosote-contaminated soil. Letters in Applied
456 Microbiology. 44**,** 293-300.
457 Guo, M., et al., 2017. Microbial mechanisms controlling the rhizosphere effect of ryegrass on degradation of polycyclic aromatic
458 hydrocarbons in an aged-contaminated agricultural soil. Soil Biology and Biochemistry. 113**,** 130-142.
459 Hannula, S. E., et al., 2012. 13C pulse-labeling assessment of the community structure of active fungi in the rhizosphere of a
460 genetically starch-modified potato (*Solanum tuberosum*) cultivar and its parental isoline. New Phytologist. 194**,** 784-
461 799.
462 Haritash, A. K., Kaushik, C. P., 2009. Biodegradation aspects of Polycyclic Aromatic Hydrocarbons (PAHs): A review. Journal
463 of Hazardous Materials. 169**,** 1-15.
464 Hayward, A. C., et al., 2010. *Stenotrophomonas* and *Lysobacter*: ubiquitous plant-associated gamma-proteobacteria of
465 developing significance in applied microbiology. Journal of Applied Microbiology. 108**,** 756-770.
466 Herrera-Jiménez, E., et al., 2018. Comparative effects of two indole-producing *Trichoderma* strains and two exogenous
467 phytohormones on the growth of *Zea mays* L., with or without tryptophan. Journal of soil science and plant nutrition.
468 18**,** 188-201.
469 Joner, E. J., Corinne, L., 2003. Rhizosphere gradients of polycyclic aromatic hydrocarbon (PAH) dissipation in two industrial
470 soils and the impact of arbuscular mycorrhiza. Environmental Science & Technology. 37**,** 2371-5.
471 Kawasaki, A., et al., 2016. Specific influence of white clover on the rhizosphere microbial community in response to polycyclic
472 aromatic hydrocarbon (PAH) contamination. Plant & Soil. 401**,** 365-379.
473 Khan, S., et al., 2013. Plant–bacteria partnerships for the remediation of hydrocarbon contaminated soils. Chemosphere. 90**,**
474 1317-1332.
475 Kong, F. X., et al., 2018. Degradation of polycyclic aromatic hydrocarbons in soil mesocosms by microbial/plant
476 bioaugmentation: Performance and mechanism. Chemosphere. 198**,** 83-91.
477 Kovtunovych, G., et al., 1999. Correlation between pectate lyase activity and ability of diazotrophic *Klebsiella oxytoca* VN 13
478 to penetrate into plant tissues. Plant & Soil. 215**,** 1-6.
479 Lehmann, A., et al., 2014. Arbuscular mycorrhizal influence on zinc nutrition in crop plants – A meta-analysis. Soil Biology &
480 Biochemistry. 69**,** 123-131.
481 Li, S. M., et al., 2013. [Diversity of arbuscular mycorrhizal fungi in special habitats: a review]. Ying Yong Sheng Tai Xue Bao.
482 24**,** 3325-3332.
483 Liu, W., et al., 2013. Rhizobacteria (*Pseudomonas* sp. SB) assist phytoremediation of oily-sludge-contaminated soil by tall fescue
484 (*Testuca arundinacea* L.). Plant & Soil. 371**,** 533-542.
485 Lozupone, C., et al., 2011. UniFrac: an effective distance metric for microbial community comparison. Isme Journal. 5**,** 169-
486 172.
487 Lu, Y., et al., 2004. Linking microbial community dynamics to rhizosphere carbon flow in a wetland rice soil. Fems Microbiology
488 Ecology. 48**,** 179-186.
489 Ma, Y., et al., 2015. The hyperaccumulator Sedum plumbizincicola harbors metal-resistant endophytic bacteria that improve its
490 phytoextraction capacity in multi-metal contaminated soil. Journal of Environmental Management. 156**,** 62-69.
491 Magoc, T., Constant penalty functions to simplify optimization of the Choquet integral under constraints. IEEE International
492 Conference on Fuzzy Systems, 2011.
493 Pérezdeluque, A., et al., 2017. The interactive effects of arbuscular mycorrhiza and plant growth-promoting rhizobacteria
494 synergistically enhance host plant defences against pathogens. Scientific Reports. 7**,** 16409.

Pacwa-Płociniczak, M., et al., 2016. Monitoring the changes in a bacterial community in petroleum-polluted soil bioaugmented with hydrocarbon-degrading strains. Applied Soil Ecology. 105**,** 76-85.

Pennisi, E., The secret life of fungi. American Association for the Advancement of Science, 2004.

Philippe, V., et al., 2007. Active root-inhabiting microbes identified by rapid incorporation of plant-derived carbon into RNA. Proc Natl Acad Sci U S A. 104**,** 16970-16975.

Potin, O., et al., 2004. Bioremediation of an aged polycyclic aromatic hydrocarbons (PAHs)-contaminated soil by filamentous fungi isolated from the soil. International Biodeterioration & Biodegradation. 54**,** 45-52.

Rao, M., et al., 2015. Isolation of polycyclic aromatic hydrocarbons degrading PGPR from a oil products contaminated site in Hyderabad, Telangana State, India. International Journal of Pharma and Biosciences. 6**,** 305-317.

Ren, C. G., et al., 2017. Enhanced phytoremediation of soils contaminated with PAHs by arbuscular mycorrhiza and rhizobium. International Journal of Phytoremediation. 19**,** 789-797.

Rillig, M. C., Steinberg, P. D., 2002. Glomalin production by an arbuscular mycorrhizal fungus: a mechanism of habitat modification? Soil Biology & Biochemistry. 34**,** 0-1374.

Rillig, M. C., et al., 2001. Large contribution of arbuscular mycorrhizal fungi to soil carbon pools in tropical forest soils. Plant & Soil. 233**,** 167-177.

Sara, G., et al., 2014. Community structure and PAH ring-hydroxylating dioxygenase genes of a marine pyrene-degrading microbial consortium. Biodegradation. 25**,** 543-556.

Sawulski, P., et al., 2014. Effects of polycyclic aromatic hydrocarbons on microbial community structure and PAH ring hydroxylating dioxygenase gene abundance in soil. Biodegradation. 25**,** 835-847.

Shahi, A., et al., 2016. Reconstruction of bacterial community structure and variation for enhanced petroleum hydrocarbons degradation through biostimulation of oil contaminated soil. Chemical Engineering Journal. 306**,** 60-66.

Shahsavari, E., et al., 2015. Rhizoremediation of phenanthrene and pyrene contaminated soil using wheat. Journal of Environmental Management. 155**,** 171-176.

Sharma, S., et al., 2005. Characterization of bacterial community structure in rhizosphere soil of grain legumes. Microbial Ecology. 49**,** 407-415.

Shi, W., et al., 2017. Effective remediation of aged HMW-PAHs polluted agricultural soil by the combination of *Fusarium* sp. and smooth bromegrass (*Bromus inermis* Leyss.). Journal of Integrative Agriculture. 16**,** 199-209.

Singleton, D. R., et al., 2011. Pyrosequence analysis of bacterial communities in aerobic bioreactors treating polycyclic aromatic hydrocarbon-contaminated soil. Biodegradation. 22**,** 1061-1073.

Smith, S. E., Read, D. J., 2010. Mycorrhizal symbiosis. Academic press.

Solísdomínguez, F. A., et al., 2011. Effect of arbuscular mycorrhizal fungi on plant biomass and the rhizosphere microbial community structure of mesquite grown in acidic lead/zinc mine tailings. Science of the Total Environment. 409**,** 1009-1016.

Sun, F. L., et al., 2016. Effect of copper on the performance and bacterial communities of activated sludge using Illumina MiSeq platforms. Chemosphere. 156**,** 212-219.

Uroz, S., et al., 2013. Functional assays and metagenomic analyses reveals differences between the microbial communities inhabiting the soil horizons of a Norway spruce plantation. Plos One. 8**,** e55929.

Verma, S. C., et al., 2001. Evaluation of plant growth promoting and colonization ability of endophytic diazotrophs from deep water rice. Journal of Biotechnology. 91**,** 127-141.

Wang, L., et al., 2016. Shifts in microbial community structure during in situ surfactant-enhanced bioremediation of polycyclic aromatic hydrocarbon-contaminated soil. Environmental Science & Pollution Research. 23**,** 14451-14461.

Wu, F. Y., et al., 2011. Phenanthrene and pyrene uptake by arbuscular mycorrhizal maize and their dissipation in soil. Journal of Hazardous Materials. 187**,** 341-347.

538 Wu, N., et al., 2009. Phenanthrene uptake by Medicago sativa L. under the influence of an arbuscular mycorrhizal fungus.
539 Environmental Pollution. 157**,** 1613-1618.
540 Yateem, Awatif, 2013. Rhizoremediation of oil-contaminated sites: a perspective on the Gulf; War environmental catastrophe
541 on the State of Kuwait. Environ Sci Pollut Res Int. 20**,** 100-107.
542 Yergeau, E., et al., 2014. Microbial expression profiles in the rhizosphere of willows depend on soil contamination. Isme Journal
543 Multidisciplinary Journal of Microbial Ecology. 8**,** 344.

545 **Tables**

546 **Table 1**

547 Growth indexes of *F. elata* in response to different treatments

Treatment	FW（g）	DW（g）	PH（cm）	TN
CK	0.23±0.01d	0.0607±0.004d	24.3±0.9d	2.7±0.6a
GV	0.29±0.01c	0.0675±0.005c	26.6±1.2c	2.3±0.6a
PS	0.43±0.02b	0.0836±0.002b	30.3±1.0b	2.7±0.6a
GVPS	0.56±0.03a	0.1177±0.003a	36.7±0.8a	3.0±0.0a

548 The data represent the mean±standard deviation of three replicates. FW means fresh weight, DW means dry weight, DW
549 means dry weight, PH means plant height, and TN means tiller number. Values in each column followed with different
550 lowercase letters (a, b, c and d) indicated significant differences between different treatments.

551

552 **Table 2**

553 The content of PHE and PYR in soil as well as roots and shoots of *F. elata* under different treatments

Treatment	PHE in soil		PYR in soil		Plant concentrations of PHE (mg • kg^{-1})		Plant concentrations of PYR (mg • kg^{-1})	
	RC (mg • kg^{-1})	DE (%)	RC (mg • kg^{-1})	DE (%)	Shoot	Root	Shoot	Root
CK	2.85±0.02a	97.10	10.12±0.12a	89.67	2.25±0.10c	35.24±0.70d	0.93±0.08d	3.74±0.21d
GV	2.85±0.03a	97.10	8.72±0.08b	91.10	2.30±0.26c	43.21±0.40c	1.40±0.13c	5.87±0.10b
PS	2.84±0.02a	97.10	8.92±0.70b	90.90	2.34±0.10b	46.21±2.12b	1.48±0.18b	4.87±0.43c
GVPS	2.46±0.07b	97.50	5.11±0.22c	94.80	2.52±0.04a	54.14±3.54a	2.50±0.19a	6.25±0.09a

554 The data represent the mean ± standard deviation of three replicates. RC means residual concentration, DE means
555 degradation efficiency, Values in each column followed with different lowercase letters (a, b, and c) indicated significant
556 differences between different treatments. The same letter within a column indicates no significant difference assessed by
557 Duncan's multiple range test ($P \leqslant 0.05$) following analysis of varianc

558

559 **Table 3**

560 Summary of sequencing date, number of operational taxonomic units (OTUs), and alpha diversity in different treatment under the pollution of PHE and PYR.

	Bacteria				Fungi			
	CK	GV	PS	GVPS	CK	GV	PS	GVPS
Total number of raw tags	207059	210277	218332	214889	292090	289128	306577	311715
Total number of clean tags	205604	208833	216889	213432	288069	277262	301930	307365
Mean number of raw tags (per sample)	69019.67±11152.14	70092.33±7485.706	72777.333±10175.39	71629.67±1165.009	97363.33±2204.543	96376±8256.634	102192.3±1807.5	103905±6356.831
Mean number of clean tags (per sample)	68534.67±10870.14	69611±7337.083	72296.333±9922.511	71144±1136.746	96023±2098.435	92420.67±8008.382	100643.3±2112.008	102455±6585.639
Total OTUs	4916	5164	5570	6327	595	649	783	825
Shannon diversity	8.195±0.342	8.176±0.445	8.426±0.224	8.640±0.150	3.762±0.153	3.795±0.391	4.203±0.319	4.113±0.288
Simpson diversity	0.991±0.003	0.985±0.008	0.992±0.002	0.992±0.001	0.863±0.019	0.849±0.027	0.894±0.013	0.846±0.055
Chao1 diversity	1976.371±278.593	2041.666±180.040	2242.989±473.870	2486.449±239.018	259.417±5.596	274.682±35.375	341.247±31.128	361.605±38.804
Ace diversity	1918.487±256.318	1987.574±177.560	2209.904±443.234	2451.972±271.607	283.638±1.677	288.165±40.010	361.482±31.444	368.293±28.812
Coverage	0.994±0.001	0.995±0.001	0.994±0.002	0.993±0.002	0.999±0.000	0.999±0.000	0.999±0.000	0.999±0.000
observed_species	1638.667±252.526	1721.333±137.027	1856.66±330.390	2109.000±130.771	198.333±11.676	216.333±17.214	261.000±17.349	275.000±4.000

561

562 **Figure legends**

563 **Fig. 1. Changes in development of AMF and PGPR quantity in response to four treatments.** Note: The error bars
564 represent the standard error, and different lowercase letters (a and b) indicated significance at $P < 0.05$**.**

565 **Fig. 2. Venn diagram of fungal (A) and bacterial (B) OTUs detected in four treatments.**

566 **Fig. 3. Relative abundances of the dominant bacterial (A, C, E) and fungal (B, D, F) taxa in four treatments at**
567 **phylum (A, B), family (C, D), and genus (E, F) level.**

568 **Fig. 4. Heatmap and dendrogram of bacteria (A) and fungi (B) based on the relative abundances of dominant genera**
569 **from different soil samples.** Note: The heatmap plot indicates the relative abundance of genera in different samples. The
570 phylogenetic tree was calculated using the neighbour-joining method. The colour intensity is proportional to the relative
571 abundance of bacterial and fungal genera.

572 **Fig. 5. PCA of the OTUs detected major variations in the bacterial (A) and fungal (B) communities in different soil**
573 **samples.**

574

575 Appendices

576 **Fig. A.1. Rarefaction curves of bacterial (A) and fungal (B) OTUs in four treatments.**

577 **Fig. A.2. Cluster analysis of the bacterial (A) and fungal (B) dominant genera in different soil samples based on**
578 **unweighted UniFrac distances.**

579

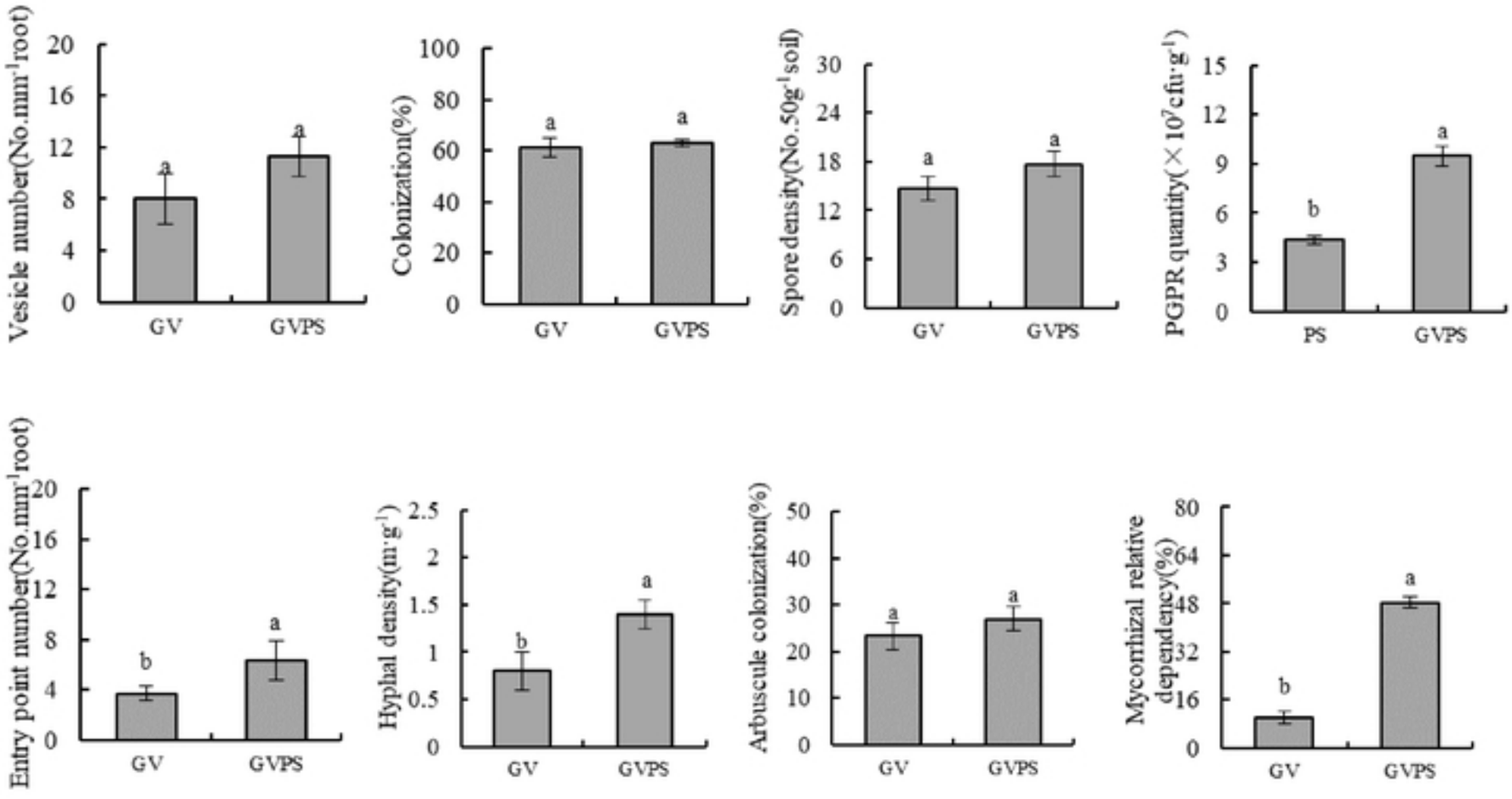
Vesicle number(No.mm-1root)
20
16
12
8
4
0
a
a
GV
GVPS
Colonization(%)
100
80
60
40
20
0
a
a
GV
GVPS
Spore density(No.50g-1soil)
30
24
18
12
6
0
a
a
GV
GVPS
PGPR quantity(×10⁷cfu·g-1)
15
12
9
6
3
0
b
a
PS
GVPS
Entry point number(No.mm-1root)
20
16
12
8
4
0
b
a
GV
GVPS
Hyphal density(m·g-1)
2.5
2
1.5
1
0.5
0
b
a
GV
GVPS
Arbuscule colonization(%)
50
40
30
20
10
0
a
a
GV
GVPS
Mycorrhizal relative dependency(%)
80
64
48
32
16
0
b
a
GV
GVPS

Figure 1

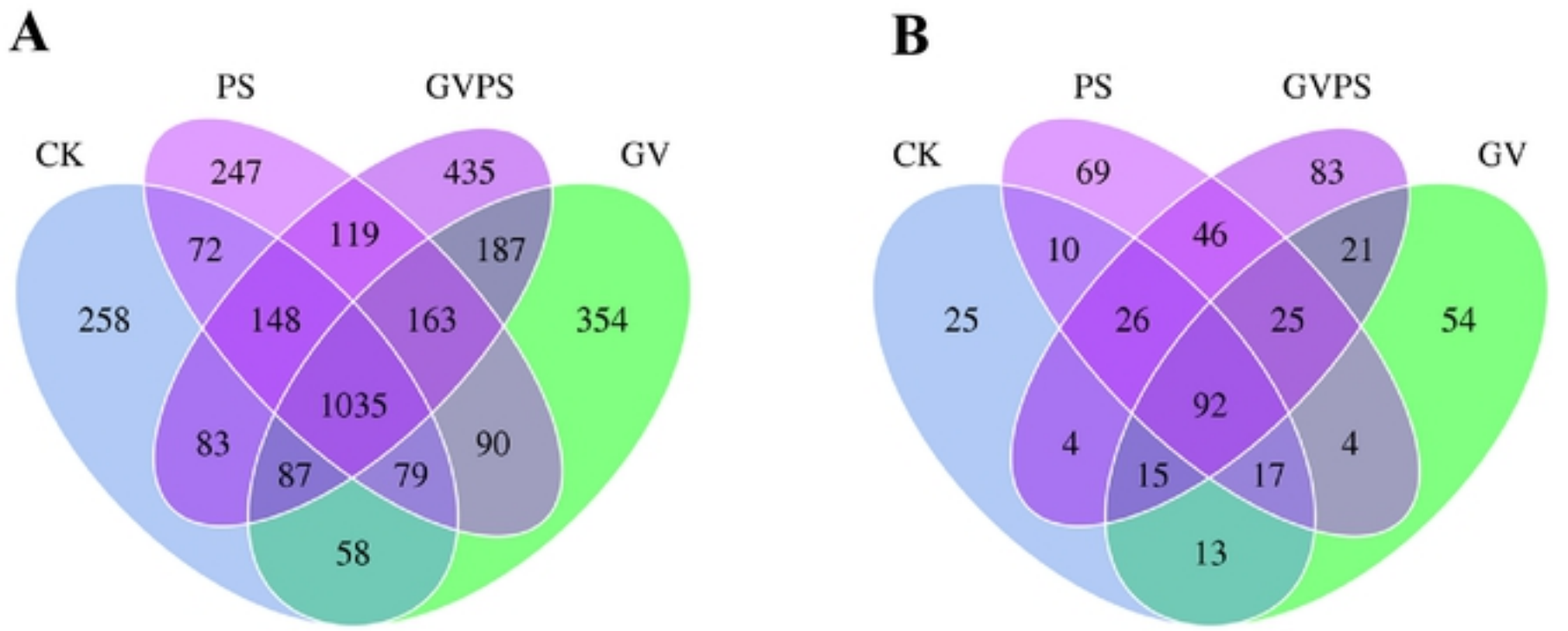

Figure 2

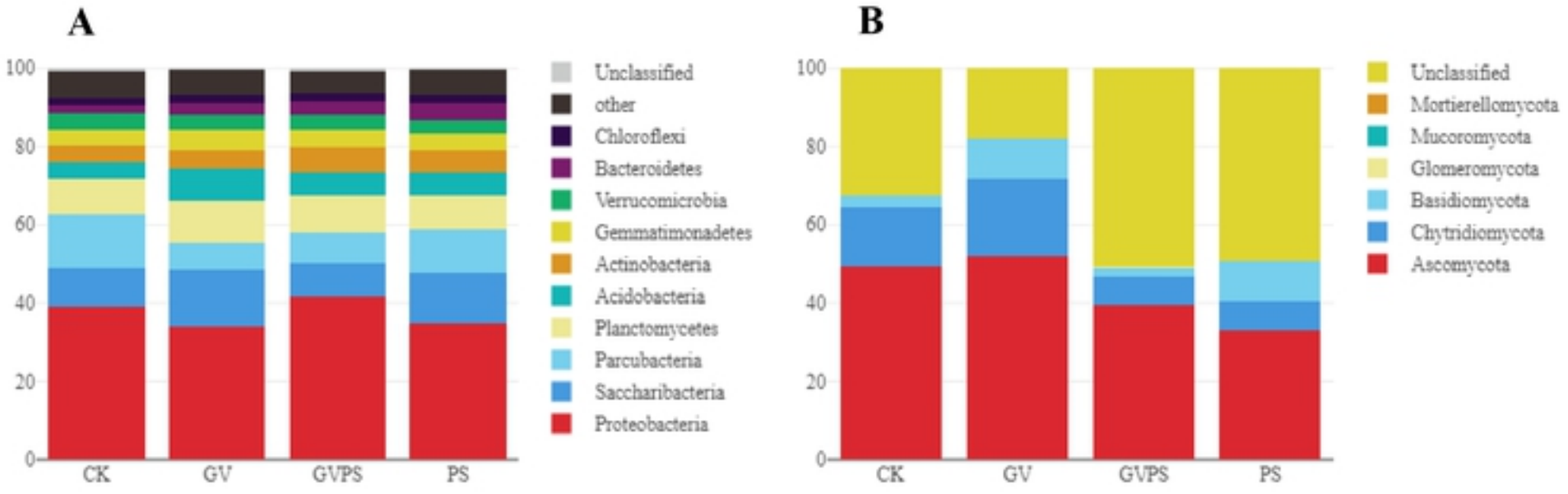
A
100
80
60
40
20
0
CK
GV
GVPS
PS
Unclassified
other
Chloroflexi
Bacteroidetes
Verrucomicrobia
Gemmatimonadetes
Actinobacteria
Acidobacteria
Planctomycetes
Parcubacteria
Saccharibacteria
Proteobacteria
B
100
80
60
40
20
0
CK
GV
GVPS
PS
Unclassified
Mortierellomycota
Mucoromycota
Glomeromycota
Basidiomycota
Chytridiomycota
Ascomycota

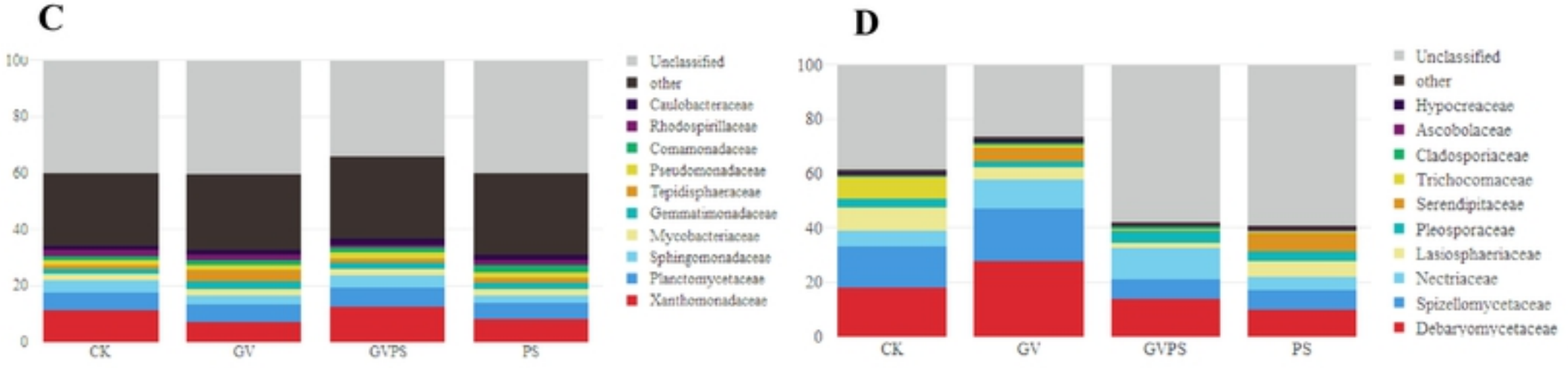
C
100
80
60
40
20
0
CK
GV
GVPS
PS
Unclassified
other
Caulobacteraceae
Rhodospirillaceae
Comamonadaceae
Pseudomonadaceae
Tepidisphaeraceae
Gemmatimonadaceae
Mycobacteriaceae
Sphingomonadaceae
Planctomycetaceae
Xanthomonadaceae
D
100
80
60
40
20
0
CK
GV
GVPS
PS
Unclassified
other
Hypocreaceae
Ascobolaceae
Cladosporiaceae
Trichocomaceae
Serendipitaceae
Pleosporaceae
Lasiosphaeriaceae
Nectriaceae
Spizellomycetaceae
Debaryomycetaceae

E

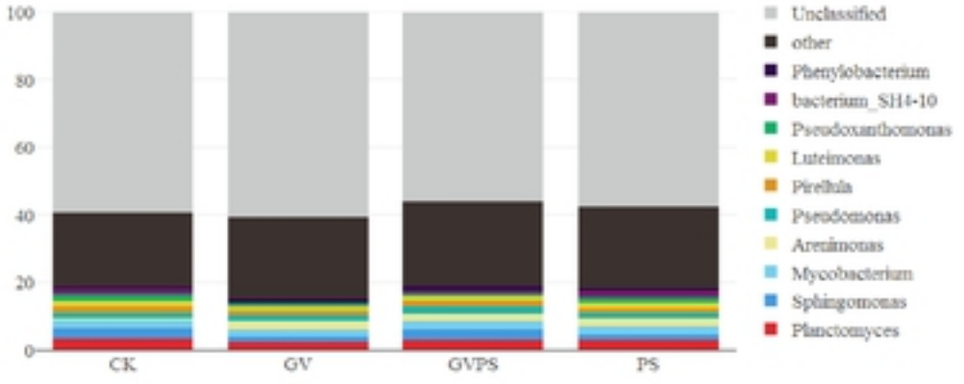
100
80
60
40
20
0
CK
GV
GVPS
PS
Unclassified
other
Phenylobacterium
bacterium_SH4-10
Pseudoxanthomonas
Luteimonas
Pirellula
Pseudomonas
Arenimonas
Mycobacterium
Sphingomonas
Planctomyces

F

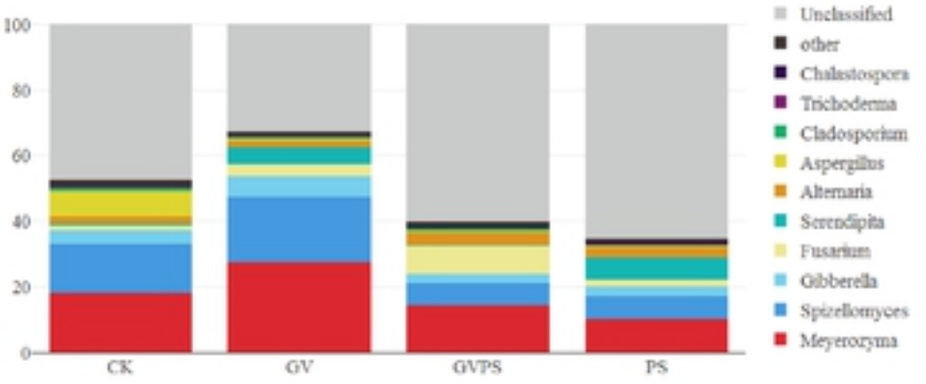
100
80
60
40
20
0
CK
GV
GVPS
PS
Unclassified
other
Chalastospora
Trichoderma
Cladosporium
Aspergillus
Alternaria
Serendipita
Fusarium
Gibberella
Spizellomyces
Meyerozyma

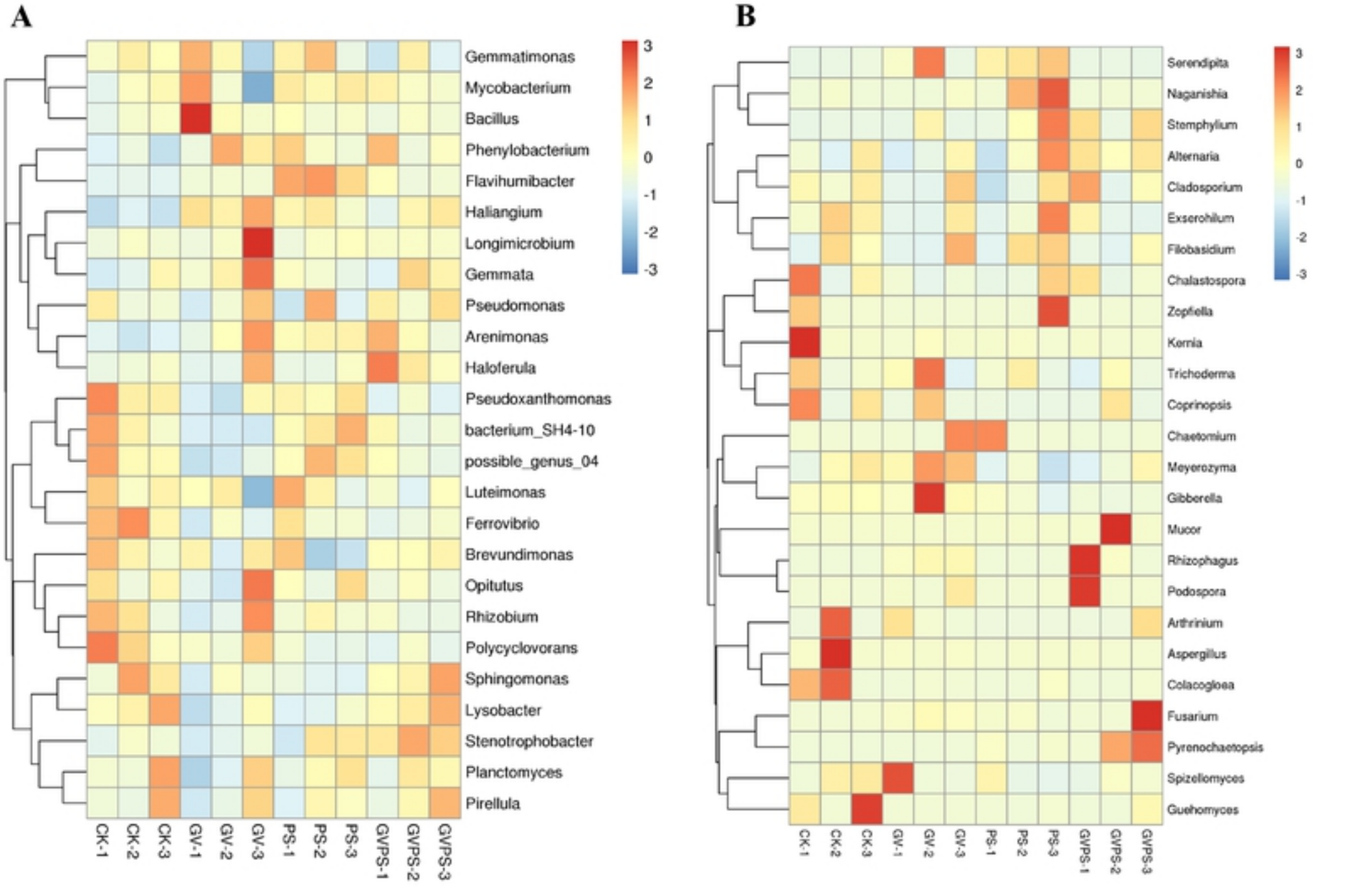
A
Gemmatimonas
Mycobacterium
Bacillus
Phenylobacterium
Flavihumibacter
Haliangium
Longimicrobium
Gemmata
Pseudomonas
Arenimonas
Haloferula
Pseudoxanthomonas
bacterium_SH4-10
possible_genus_04
Luteimonas
Ferrovibrio
Brevundimonas
Opitutus
Rhizobium
Polycyclovorans
Sphingomonas
Lysobacter
Stenotrophobacter
Planctomyces
Pirellula
3
2
1
0
-1
-2
-3
CK-1
CK-2
CK-3
GV-1
GV-2
GV-3
PS-1
PS-2
PS-3
GVPS-1
GVPS-2
GVPS-3
B
Serendipita
Naganishia
Stemphylium
Alternaria
Cladosporium
Exserohilum
Filobasidium
Chalastospora
Zopfiella
Kernia
Trichoderma
Coprinopsis
Chaetomium
Meyerozyma
Gibberella
Mucor
Rhizophagus
Podospora
Arthrinium
Aspergillus
Colacogloea
Fusarium
Pyrenochaetopsis
Spizellomyces
Guehomyces
3
2
1
0
-1
-2
-3
CK-1
CK-2
CK-3
GV-1
GV-2
GV-3
PS-1
PS-2
PS-3
GVPS-1
GVPS-2
GVPS-3

Figure 4

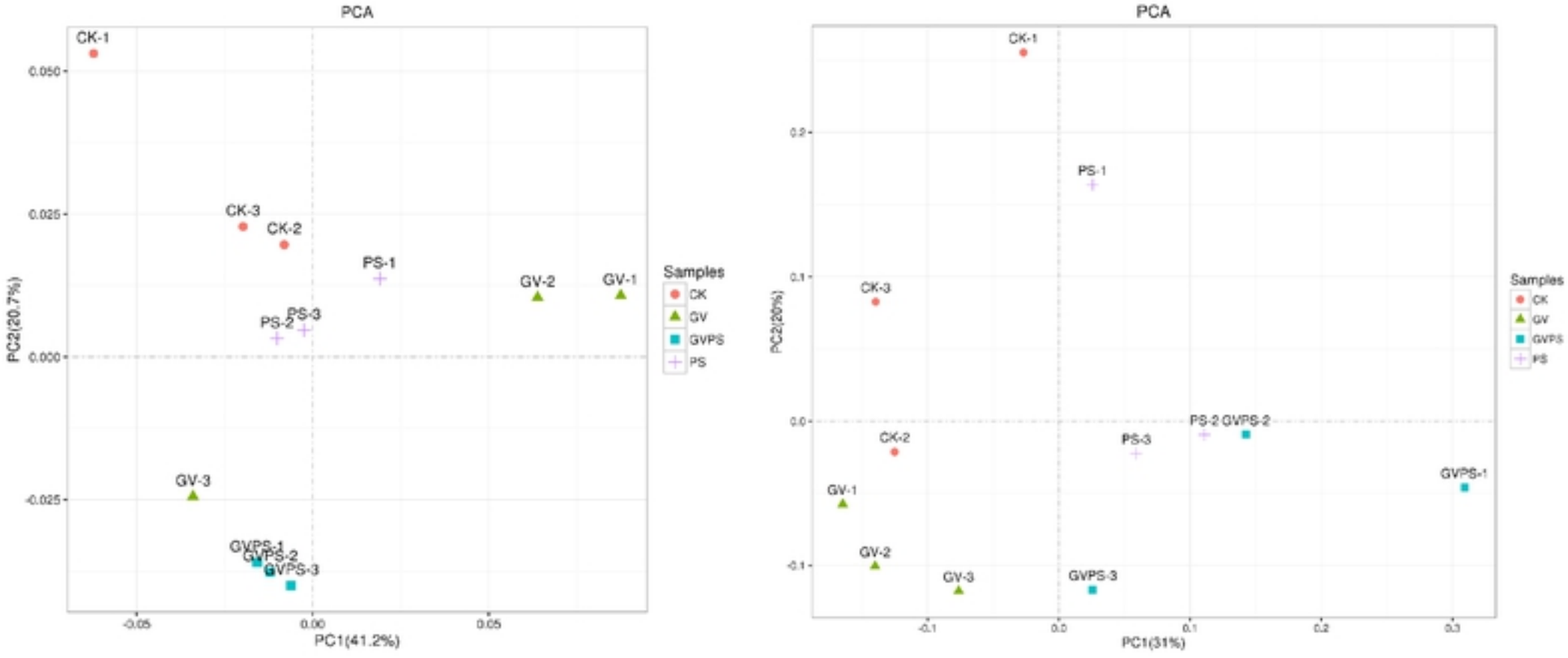
PCA
CK-1
CK-3
CK-2
PS-1
GV-2
GV-1
PS-3
PS-2
GV-3
GVPS-1
GVPS-2
GVPS-3
0.050
0.025
0.000
-0.025
-0.05
0.00
0.05
PC2(20.7%)
PC1(41.2%)
Samples
CK
GV
GVPS
PS
PCA
CK-1
PS-1
CK-3
CK-2
PS-3
PS-2
GVPS-2
GVPS-1
GV-1
GV-2
GV-3
GVPS-3
0.2
0.1
0.0
-0.1
-0.1
0.0
0.1
0.2
0.3
PC2(20%)
PC1(31%)
Samples
CK
GV
GVPS
PS

Figure 5